Title

High efficient electrical stimulation of hippocampal slices with vertically aligned carbon nanofiber microbrush array

Journal

Biomedical Microdevices: BioMEMS and Biomedical Nanotechnology, 11(4)

ISSN

1572-8781

Authors

de Asis, Edward D.
Nguyen-Vu, T. D.
Arumugam, Prabhu U.
et al.

Publication Date

2009-08-01

DOI

10.1007/s10544-009-9295-7

Peer reviewed

Biomed Microdevices (2009) 11:801–808
DOI 10.1007/s10544-009-9295-7

High efficient electrical stimulation of hippocampal slices with vertically aligned carbon nanofiber microbrush array

Edward D. de Asis Jr. · T. D. Barbara Nguyen-Vu · Prabhu U. Arumugam · Hua Chen · Alan M. Cassell · Russell J. Andrews · Cary Y. Yang · Jun Li

Published online: 17 March 2009

Abstract Long-term neuroprostheses for functional electrical stimulation must efficiently stimulate tissue without electrolyzing water and raising the extracellular pH to toxic levels. Comparison of the stimulation efficiency of tungsten wire electrodes (W wires), platinum microelectrode arrays (PtMEA), as-grown vertically aligned carbon nanofiber microbrush arrays (VACNF MBAs), and polypyrrole coated (PPy-coated) VACNF MBAs in eliciting field potentials in the hippocampus slice indicates that, at low stimulating voltages that preclude the electrolysis of water, only the PPy-coated VACNF MBA is able to stimulate the CA3 to CA1 pathway. Unlike the W wires, PtMEA, as-grown VACNF MBA, and the PPy-coated VACNF MBA elicit only excitatory postsynaptic potentials (EPSPs). Furthermore, the PPy-coated VACNF MBA evokes somatic action potentials in addition to EPSPs. These results highlight the PPy-coated VACNF's advantages in lower electrode impedance, ability to stimulate tissue through a biocompatible chloride flux, and stable vertical alignment in liquid that enables access to spatially confined regions of neuronal cells.

Keywords Vertically aligned carbon nanofiber · Electrical stimulation · Neural electrical interface · Hippocampal brain slice · Neural recording

E. D. de Asis Jr.
Departments of Electrical Engineering and Bioengineering,
Santa Clara University,
500 El Camino Real,
Santa Clara, CA 95053, USA

T. D. B. Nguyen-Vu
Department of Molecular Cell Physiology,
Stanford University Medical School,
Palo Alto, CA 94305, USA

P. U. Arumugam · H. Chen
ELORET Corporation, NASA Ames Research Center,
Moffett Field, CA 94035, USA

A. M. Cassell
University Affiliated Research Center, University of California,
Santa Cruz,
Moffett Field, CA 94035, USA

R. J. Andrews · J. Li
NASA Ames Research Center,
Moffett Field, CA 94035, USA

C. Y. Yang
Center for Nanostructures, Santa Clara University,
500 El Camino Real,
Santa Clara, CA 95053, USA

Present address:
J. Li (✉)
Department of Chemistry, Kansas State University,
Manhattan, KS 66506–0401, USA
e-mail: junli@ksu.edu

1 Introduction

Functional electrical stimulation (FES) methods such as deep brain stimulation (DBS) have been used to treat neuropathological disorders such as Parkinson's Disease, epilepsy, schizophrenia, and obsessive compulsive disorder (Snyder and Robinson 2000; Cameron et al. 2004; Mayberg et al. 2005). In neuroelectronics research toward these applications, planar microelectrode arrays (MEA) are commonly used for stimulation and recording of acute (Heuschkel et al. 2002) and organotypic (Glomieh et al. 2006) brain slices as well as dissociated neuronal cell cultures (Nam et al. 2006; Soussou et al. 2007). In previous

studies, we have demonstrated that vertically aligned carbon nanofiber (VACNF) microbrush arrays (MBAs) are ideal for long-term implantation because: (1) The neural electrical interface (NEI) provided by the three-dimensional (3-D) open structure of VACNF presents a much lower impedance compared to planar metal electrodes; (2) The CNF backbone provides mechanical stability for interfacing with neural tissues; and (3) Coating CNFs with an electrically conductive polymer (ECP) can improve the biocompatibility of the electrodes (Nguyen-Vu et al. 2006). We have shown that the VACNF architecture is a novel nanostructured substrate for culturing networks of neuron-like pheochromocytoma cells (PC12) (Nguyen-Vu et al. 2007). However, using VACNF MBAs for electrical stimulation of neural tissues has not been demonstrated. A major criterion for a chronic implantable neural stimulation device is the safe delivery of current or voltage stimulus to the neural tissue without electrolyzing water (Merrill et al. 2005). Recent studies have demonstrated the feasibility of using entangled single-walled carbon nanotube (SWNT) towers for stimulating cultured hippocampal neurons (Wang et al. 2006) and individual VACNFs for stimulating organotypic hippocampal slices (Yu et al. 2007). While these results are encouraging, the unique advantages of the 3-D nanostructure of CNT towers or VACNFs over planar MEAs remain to be demonstrated. In this study, we show that a 3-D VACNF MBA coated with conformal ECP, i.e. polypyrrole (PPy; Abidian et al. 2006; Cui et al. 2003; Kim et al. 2004), can indeed stimulate acute hippocampal brain slices at a very low voltage without electrolyzing water. We utilized the Schaffer collateral pathway of CA3 to CA1 in the hippocampus for the stimulation experiments (Lorente de No 1934; Butler and Hodos 2005). The PPy-coated VACNF MBA has been systematically compared with a pair of tungsten wire electrodes, a planar platinum MEA, and an as-grown VACNF MBA. We demonstrate that the PPy-coated VACNF MBA elicits the largest amplitude in evoked field potentials. Its effective stimulation of hippocampal slices is likely due to the unique freestanding brush-like 3D nanostructure. Most importantly, it generates a fast field potential waveform that is not observed when stimulating with the other three electrode types. We attribute this to the ability of some vertical CNFs to access spatially limited regions proximal to the soma. Even for the common slow field potential wave, our results suggest that, compared to stimulation applied by the traditional Pt MEA and as-grown VACNF MBA which can lead to a harmful and toxic extracellular pH change that causes cell death, the PPy-coated VACNF MBA stimulates cells through an extracellular chloride flux that not only amplifies the amplitude but also elongates the duration of evoked field potentials. The PPy-coated VACNF MBA is potentially a novel biocompatible electrode for chronic implantable devices with enhanced quiescent neurophysiological signals under electrical stimulation.

2 Experimental

2.1 Preparation of rat hippocampal slices

Acute slices were prepared from 1 to 2 month old male Wistar rat weighing approximately 100 to 125 g in accordance with the animal experiment protocol approved by the Institution Animal Care and Use Committee at NASA Ames Research Center. The rat was anesthetized using 3 ml isofluorane (Aerrane), decapitated, and 400–500 μm thick transverse hippocampal slices were excised from brain tissue. Prior to the electrophysiological measurements, the hippocampal slices cut using a Stoelting Chopper were stored in oxygenated artificial cerebrospinal fluid (ACSF, 119 mM NaCl, 11 mM D-(+)-Glucose, 2.5 mM $CaCl_2.H_2O$, 2.5 mM KCl, 1.3 mM $MgSO_4$, 1 mM NaH_2PO_4, 26.2 mM $NaHCO_3$) for 1 h to recover.

2.2 Fabrication of electrode arrays

The hippocampal slices were stimulated using W wires, Pt MEA, an as-grown VACNF MBA, and PPy-coated VACNF MBA. The Pt MEA including the electrode footprint, interconnects, and peripheral bonding pads (Fig. 1(a)) was fabricated with a lift-off process by depositing a 200 nm thick Pt layer on a lithographically patterned Si wafer which was covered with 400 nm thick silicon nitride. The resistance as measured between the electrodes and contact pads was approximately 800 Ω. A 400 nm silicon nitride layer was deposited over the electrode array via plasma enhanced chemical vapour deposition (PECVD) using silane (SH_4, 2,000 sccm) and ammonia (NH_3, 33.5 sccm) at a pressure of 250 mTorr and a temperature of 350°C. Windows in the nitride were defined over the electrodes and the contact pads via photolithography using a 1.6 μm thick Shipley 3612 resist and opened via an 80-s sulphur hexafluoride (SF_6, 25 sccm) reactive ion etch (RIE) at 125 W and 200 mTorr. Fabrication of the as-grown VACNF MBA and PPy-coated VACNF MBA followed the similar process steps outlined for the Pt MEA except that Cr or Ti was used to form the interconnects, bonding pads, and electrodes. A 30 nm thick nickel catalyst layer was deposited with an ion beam sputter on the electrode area. CNFs were grown via PECVD using a C_2H_2 feedstock (22.5 sccm) and NH_3 diluent (80 sccm) at a processing pressure of 4 Torr and processing temperature of 725°C for 10 min resulting in VACNF with the length ranging from 2 to 4 μm and the diameter ranging from 100

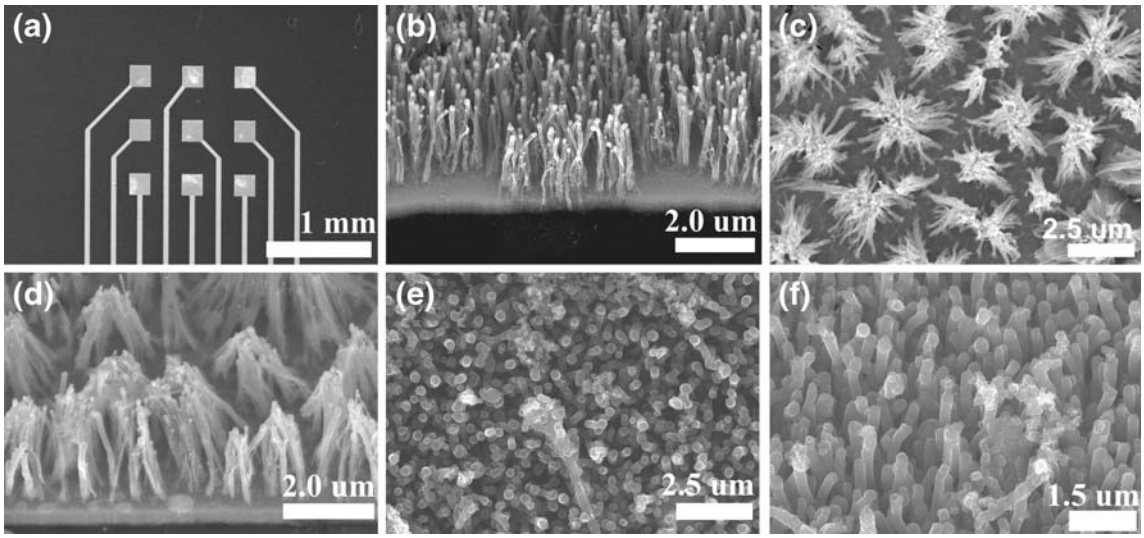

Fig. 1 SEM micrograph of electrode arrays: (**a**) the layout of the 3×3 electrode array; (**b**) as-grown VACNFs on electrodes at 45° perspective view; the formation of microbundles of the same sample after dipping into solution and then dried in the air with (**c**) top view and (**d**) 45° perspective view; and a similar sample after PPy coating in solution and then dried in the air with (**e**) top view and (**f**) 45° perspective view

to 250 nm (Cruden et al. 2003). Nickel catalyst particles located at the tips were removed via an etch in 1 M nitric acid. PPy was electrochemically deposited using an Autolab potentiostat (Echochemie Co., The Netherlands) from pyrrole (50 mM) in KCl (1.0 M) at 1.50 V (vs. Ag/AgCl (3 M KCl)) for 120 s (Nguyen-Vu et al. 2006).

2.3 Stimulation protocol and electrophysiology

To stimulate the tissue, a monophasic current pulse from a stimulation isolation unit (World Precision Instruments SIU A320R) was applied. Although biphasic current waveforms are known to deliver better charge balance (Merrill et al. 2005), the monophasic current pulse was adequate for this study. The SIU was triggered using a Grass Stimulator (Astro-Med, Inc. S48J stimulator). Stimulation using W wires was applied at the Schaffer Collateral (SC). Stimulation of the hippocampal brain slices using the Pt MEA, as-grown VACNF MBA, and the PPy-coated VACNF MBA was applied with the following procedure: The slices were laid flat against the electrode array as shown in Fig. 2 and current was applied between electrodes 8 and 9. The

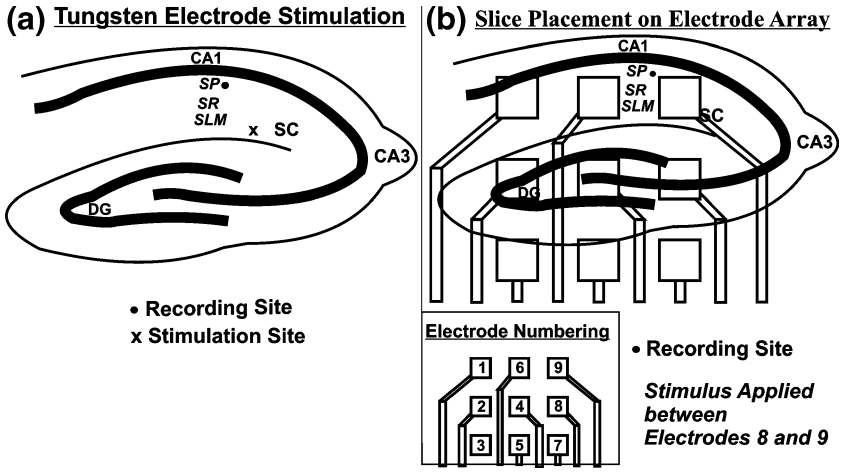

Fig. 2 Set-up for stimulating rat hippocampal brain slices. (**a**) Location of stimulation and recording sites on a hippocampal slice when stimulating using tungsten wire electrodes. (**b**) Placement of the hippocampal slice on a 3×3 electrode array. Inset: electrode numbering convention. *DG* Dentate Gyrus, *SC* Schaffer Collateral, *CA1* Cornus Ammonis 1, *CA 3* Cornus Ammonis 3, *SP* Striatum Pyramidale, *SR* Striatum Radiatum, *SLM* Striatum Lacunosum Moleculare

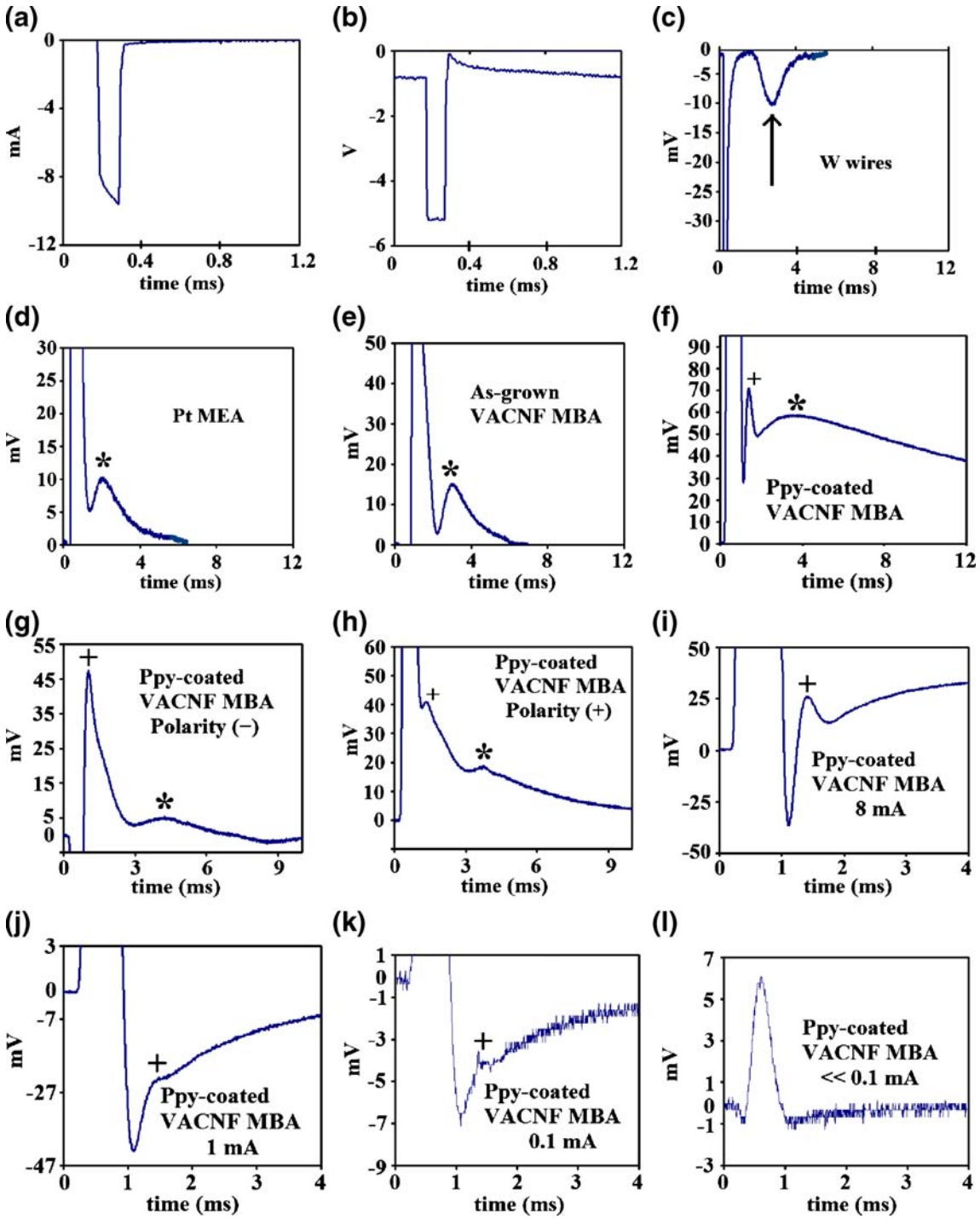

Fig. 3 Recorded waveforms of (**a**) stimulating current artifact waveform, (**b**) stimulating electrode voltage waveform. Field potentials recorded in response to the 10.5 mA stimulating currents with (**c**) tungsten wire electrodes, (**d**) Pt MEA, (**e**) as-grown VACNF MBA, (**f**) PPy-coated CNF MBA. Field potential in response to stimulation applied with PPy-coated CNF MBA at (**g**) negative polarity and (**h**) positive polarity. Recorded field potential elicited by current stimulation applied with PPy-coated VACNF MBA as in (**f**) with (**i**) I_{stim}= 8 mA, (**j**) I_{stim}=1 mA, (**k**) I_{stim}=0.1 mA, and (**l**) I_{stim}<<0.1 mA. *Arrows* denote excitatory field potentials. *Asterisk* denotes long duration field potentials. *Plus sign* denotes short duration field potentials

applied stimulus consisted of a 100 μs pulse applied at a rate of 5.2 pulses/s (Fig. 3(a)). The response was recorded from the striatum pyramidale (SP) of CA1 using an extracellular glass micropipette electrode filled with 2 M NaCl. The access resistance of the micropipette electrode was measured to be approximately 1–3 MΩ. The recorded response was amplified and filtered using a GeneClamp 500 B patch clamp amplifier configured to provide a gain

of 10 *V*/*V* and lowpass filtering provided by a Bessel Filter with a cutoff frequency of 1 kHz.

3 Results and discussion

3.1 Recorded evoked bioelectrical signals from hippocampal slices

The stimulating current, voltage waveform, and the corresponding evoked field potential response for a 10.5 mA stimulation pulse using W wires, Pt MEA, as-grown VACNF MBA, and PPy-coated VACNF MBA are shown in Fig. 3(a–f). The total response consisted of the evoked extracellular field potential recorded at SP superimposed upon the stimulus artifact. The typical response to a stimulus applied using W wires consisted of a negative going field potential of 3 ms duration and a latency of 3 ms. The typical observed responses to a stimulus applied using a Pt MEA and an as-grown VACNF MBA consisted of a positive going field potential with a similar duration (4 ms) and latency (2.5–3 ms). However, the responses to a stimulus applied using a PPy-coated VACNF MBA is dramatically different. The results show two components, i.e. a narrow field potential spike (of 1 ms duration) with a peak latency of 1.3 ms on top of a longer field potential wave (20–25 ms duration) with a peak latency of 3.7–4 ms.

To ascertain that the observed field potentials were real cellular responses instead of artifacts, the polarity of the applied current pulse was reversed on the SIU while all other parameters were the same. The two components of the evoked field potential under stimulation with the PPy-coated VACNF MBA were always found to be positive and appeared at the same latency with similar durations regardless of polarity of the applied current pulse (Fig. 3(g, h)). These results indicate that the recorded field potentials were indeed biological responses.

3.2 Comparison of stimulation efficiencies of W wires, Pt MEA, As-grown VACNF MBA, and PPy-coated VACNF MBA

To assess and compare the performance of W wires, Pt MEA, as-grown VACNF MBA, and PPy-coated VACNF MBA, an input versus output curve was generated measuring the field potential amplitude as the stimulus current was progressively decreased from 10 to 1 mA in 1 mA increments and then from 1 to 0 mA in 100 μA increments. The effective stimulus output, as measured by the voltage excursion between to the two electrode poles, was also recorded for each stimulus level. The amplitude of the field potential was estimated to be the difference between the voltage at the peak of the evoked potential and the baseline after subtracting the stimulus artifact. Example traces of the recorded field potential in response to different stimulus intensity applied using the PPy-coated VACNF MBA is illustrated in Figs. 3(i–l).

The average stimulating electrode voltage and average field potential amplitude recorded over two brain slices for the W wires, four slices for the Pt MEA and as-grown VACNF MBA, and five slices for the PPy-coated VACNF MBA versus the amplitude of the stimulation current pulse is plotted in Fig. 4. Clearly, the W wires, Pt MEA, and as-grown VACNF MBA all failed to evoke cellular responses at stimulating current pulse amplitudes below 1 mA (Fig. 4(b, d)). Only the PPy-coated VACNF MBA was able to elicit a cellular response at such weak stimulation and showed both the fast and slow waves. At the stimulating current above 2 mA, field potential waves can be measured with all four types of electrodes but with varied amplitude. Meanwhile, the electrode voltages with the W electrodes and Pt MEA are measured much higher than that on PPy-coated VACNF MBA (Fig. 4(a, c)). The voltages of as-grown VACNF MBA were slightly lower than the PPy-coated VACNF MBA, but it failed to generate the cellular response (i.e. no evoked field potential waves) below 1 mA. Only the PPy-coated VACNF MBA were able to effectively stimulate the hippocampal slice at a current pulse

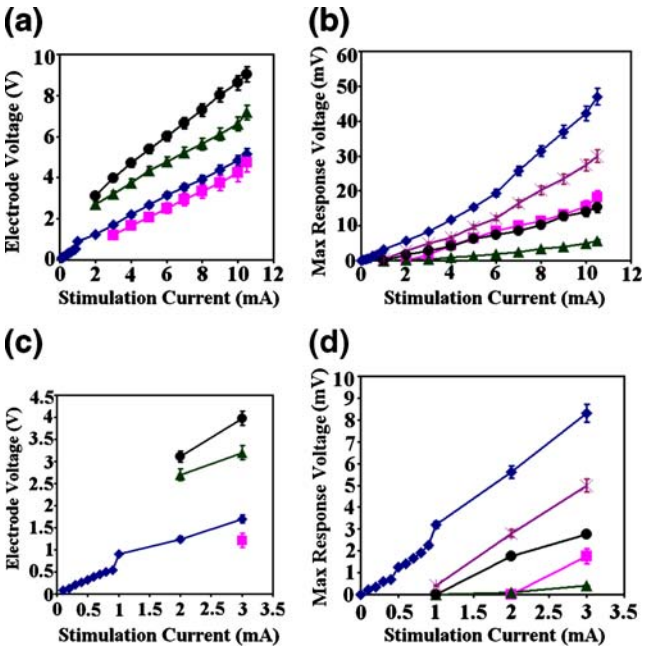

Fig. 4 (**a**) Electrode voltage and (**b**) response amplitude of field potential vs. the stimulation current. (**c**) and (**d**) are enlarged plots of (**a**) and (**b**) at low currents, respectively. *Error bars* ≈ ± Standard Deviation. *Filled diamonds* PPy-coated VACNF MBA (in (**b**) and (**d**): corresponding to amplitude of short duration field potential), *multiplication signs* Amplitude of long duration field potential elicited by PPy-coated VACNF MBA, *filled circles* Tungsten electrodes, *filled square* As-Grown VACNF MBA, *filled triangle* Pt MEA

less than 1 mA and an electrode voltage less than 1 V (a safe value without inducing electrolysis of water).

3.3 Connection between recorded evoked electrical signals and differences in electrode structure

CA1 receives synaptic input from both SC and PP (Empson and Heinemann 1995; Yu et al. 2001; Levy et al. 1998; Nathan and Lambert 1991; Biscoe and Duchen 1985; Arrigoni and Greene 2004; Staff and Spruston 2003). Because of the small electrode size (10 μm in diameter) and the ability to penetrate into the thick brain tissue, the stimulation by W wires is localized to the SC pathway only; thus, generating the negative going field potential consisting of the summation of excitatory postsynaptic potentials (EPSPs) at CA1 evoked by stimulation at the SC (Dingledine et al. 1986; Tominaga et al. 2002). The mean amplitude of the excitatory field potential was 15.25 mV at a stimulation current of 10.5 mA. Stimulation by the Pt MEA evoked a long duration positive-going field potential with mean amplitude of 5.75 mV at a stimulation current of 10.5 mA. Stimulation by the as-grown VACNF MBA elicited a long duration positive going field potential with the mean amplitude increased to 18.2 mV at a stimulation current of 10.5 mA. Stimulation by the PPy-coated VACNF MBA evoked a short duration positive-going field potential followed by a long duration positive-going field potential. At a stimulation current of 10.5 mA, the mean amplitude of the short duration positive-going field potential was at a remarkably large value of 47 mV. Clearly, the PPy-coated VACNF MBA elicited the strongest cellular response (Fig. 4). This is likely due to the unique vertical brush-like nanostructured enabled by enhanced mechanical stability of the VACNF arrays with PPy coating (Fig. 1). Upon drying after wet treatment, the as-grown VACNF MBA electrodes collapse into microbundles due to the strong cohesive capillary force (Nguyen-Vu et al. 2006; Nguyen-Vu et al 2007).The PPy coating relieves this problem so that the CNFs retain their freestanding vertical alignment. The PPy coating also has slight positive charges which promote the adhesion of the brain slice to the electrode.

The latency of the evoked field potential under stimulation with the four types of electrode carries important information. The positive-going field potentials evoked by the Pt MEA and as-grown VACNF MBA have similar latency as the slow field potential evoked by the PPy-coated VACNF MBA, i.e. 2.5–4 ms, but the duration is much shorter (2–4 vs. 20–25 ms). In the field potential waveforms evoked by the PPy-coated VACNF MBA, the short duration field potential is less sensitive to the current stimulus amplitude compared to the long duration field potential in that the long duration field potential disappears at a higher current stimulus amplitude compared to the short field potential. Furthermore, under any stimulating current evoking both field potentials, the amplitude of the short duration field potential is larger than that of the long duration one and the duration is much smaller. These observations agree with the results discussed by Dingledine et al. (Dingledine et al. 1986) and Tominaga et al. (Tominaga et al. 2002) who observed short duration somatic action potentials superimposed upon a long duration voltage-dependent postsynaptic depolarization. The Pt MEA, the as-grown VACNF MBA, and the PPy-coated VACNF MBA are all able to evoke a slow duration voltage-dependent field potential which corresponds to the NMDA-mediated voltage-dependent postsynaptic depolarization of a population of SP neurons (Dingledine et al. 1986). Only the PPy-coated VACNF MBA is able to elicit the short duration field potential which consists of the somatic action potentials observed by Dingledine et al (Dingledine et al. 1986).

The electrode footprint for the three electrode arrays are the same; however, the VACNF on both the as-grown VACNF MBA and the PPy-coated VACNF MBA are three dimensional conductors that vastly increase the electrode surface area leading to a reduced interface impedance compared to the Pt MEA. The polypyrrole coating on the PPy-coated VACNF MBA adds a pseudocapacitance to the electrode impedance further reducing the electrode impedance so that it can deliver a larger current at the same electrode voltage compared to the as-grown VACNF MBA (Nguyen-Vu et al. 2006). The larger current elicits a larger amplitude postsynaptic depolarization of neurons in SP by reducing the probability of cationic block of NMDA channels (Dingledine et al. 1986). Furthermore, the PPy coating is positively charged with improved tissue-electrode adhesion. The freestanding needle-shaped VACNFs are able to penetrate into the tissue and access the cell body to elicit somatic action potentials. Thus, the difference in evoked field potentials between the Pt MEA, the as-grown VACNF MBA, and the PPy-coated VACNF MBA highlight the ability of the well-separated freestanding VACNFs to elicit larger amplitude field potentials and access the perisomatic region of pyramidal cells in SP.

The observed responses also underscore the different electrochemical mechanisms through which the Pt MEA, the as-grown VACNF MBA, and the PPy-coated VACNF MBA stimulate cells. Our results suggest that the Pt MEA and the as-grown VACNF MBA electrolyze water leading to a H^+ and OH^- flux which has no effect on the membrane potential. Stimulation applied by PPy-coated VACNF MBA leads to a chloride flux that transiently increases the extracellular chloride concentration in the dendritic arbors and the spatially confined perisomatic regions. The

increased chloride concentration depolarizes the postynaptic membrane removing the Mg^{2+} block of individual NMDA ion channels boosting the amplitude and prolonging the duration of the postynaptic depolarization. In the soma, the increased chloride concentration and resulting membrane depolarization brings the membrane closer to threshold facilitating action potentials comprising the large amplitude, short duration field potential.

Compared to the recorded evoked field potentials described in the literature (Heuschkel et al. 2002; Glomieh et al. 2006; Nam et al. 2006; Soussou et al. 2007; Yu et al. 2007), the amplitude of the recorded field potential evoked using our PPy-coated VACNF MBA was much larger. However, in references (Nam et al. 2006; Soussou et al. 2007), the stimulus was applied to a dissociated hippocampal cell culture. In our experiment, stimulus was applied to an acute brain slice. The area of the electrodes in the PPy-coated VACNF MBA was also much larger than in previous studies (Glomieh et al. 2006; Nam et al. 2006; Yu et al. 2007). Therefore, it is inconclusive to compare the stimulating efficiency through the amplitude of evoked field potentials. Interestingly, the observed field potential in Fig. 4(b) monotonically increases with stimulating current, unlike the sigmoidal stimulation curve observed in reference (Yu et al. 2007). This may be due to the fact that we use acute hippocampal slice instead of organotypic slices and the larger electrode footprint. A smaller electrode may stimulate a limited number of cells which leads to saturation of the stimulation curve at high stimulating currents. The stimulation is below the saturation level in our study.

4 Conclusions

In summary, we compared the performance of Pt MEA, as-grown VACNF MBA, and PPy-coated VACNF MBA in stimulating neurons in rat hippocampal brain slices. All three MEAs elicit a long-duration field potential; however, only the PPy-coated VACNF MBA can evoke a large-amplitude, short duration field potential with smaller latency and successfully stimulate field potentials at a much lower electrode voltage, completely avoiding electrolysis of water. Furthermore, unlike the Pt MEA and as-grown VACNF MBA in which an applied stimulus voltage is accompanied by an extracellular pH change that is highly toxic to cells, the PPy-coated VACNF MBA stimulates cells through a transient flux of chloride ions which are intrinsic to the extracellular fluid and, thus, are non-toxic and which can boost the amplitude and duration of evoked field potentials. Thus, the PPy-coated VACNF MBA can be used to safely stimulate neural tissue and enhance evoked electrical activity. Furthermore, the PPy-coating preserves the well-separated and free-standing structure of VACNF MBAs and this mechanical stability in combination with the positively charged PPy backbone and the associated chloride flux facilitate the accessibility of the PPy-coated VACNF MBA to synapses located in spatially confined synapses and perisomatic regions of the cells. Therefore, our PPy-coated VACNF MBA represents a novel, biocompatible platform for chronic implantable neuroprostheses for neural stimulation.

Acknowledgement We would like to acknowledge the support by National Institute of Neurological Disorders and Stroke (NINDS) under grant no. 1 R21 NS047721-01A1. Alan Cassell and Prabhu U Arumugam were with the University Affiliated Research Center (UARC) at NASA Ames operated by the University of California, Santa Cruz. Prabhu U Arumugam and Hua Chen are employed by the Eloret Corporation and their work is supported by a subcontract from the UARC.

References

M.R. Abidian, D. Kim, D.C. Martin, Adv. Mater. **18**, 405–409 (2006) doi:10.1002/adma.200501726
E. Arrigoni, R.W. Greene, Br. J. Pharm. **142**, 317–322 (2004) doi:10.1038/sj.bjp.0705744
T.J. Biscoe, M.R. Duchen, J. Exp. Physiol. **70**, 189–202 (1985)
A.B. Butler, W. Hodos, *Comparative Vertebrate Neuroanatomy Evolution and Adaptation*, 2nd edn. (Wiley, New Jersey, 2005)
C.M. Cameron, M. Savasta, B.L. Walter, J.L. Vitek, J. Clin. Neurosci. **21**, 40–50 (2004)
B.A. Cruden, A.M. Cassell, Q. Ye, M. Meyyappan, J. Appl. Phys. **94**, 4070–4078 (2003)
X. Cui, J. Wiler, M. Dzaman, R. Altschuler, D.C. Martin, Biomater. **24**, 777–787 (2003)
R. Dingledine, M.A. Hynes, G.L. King, J. Physiol. **380**, 175–189 (1986)
R.M. Empson, U. Heinemann, J. Physiol. **484.3**, 707–720 (1995)
G. Glomieh, W. Soussou, M. Han, A. Ahuja, M.C. Hsiao, D. Sond, A. R. Tanguay, T.W. Berger, J. Neurosci. Methods. **152**, 116–129 (2006)
M.O. Heuschkel, M. Fejtl, M. Raggenbass, D. Bertran, P. Renaud, J. Neurosci. Methods. **114**, 135–148 (2002)
D. Kim, M. Abidian, D.C. Martin, J. Biomed. Mat. Res. **4**, 577–585 (2004)
W.B. Levy, N.L. Desmond, D.X. Zhang, Learn. Memory **4**, 510–518 (1998)
R. Lorente de No, J. Psychol. Neurol. **46**, 113–117 (1934)
H.S. Mayberg, A.M. Lozano, V. Voon, H.E. McNeely, D. Seminowicz, C. Hamani, J.M. Schwalb, S.H. Kennedy, Neuron. **5**, 651–660 (2005)
D.R. Merrill, M. Bikson, J.G.R. Jefferys, J. Neurosci. Methods. **141**, 171–198 (2005)

Y. Nam, B.C. Wheeler, M.O. Heuschkel, J. Neurosci. Methods. **155**, 296–299 (2006)
T. Nathan, J.D.C. Lambert, J. Neurophysiol. **55**(5), 1704–1715 (1991)
T.D.B. Nguyen-Vu, H. Chen, A.M. Cassell, R. Andrews, M. Meyyappan, J. Li, Small **2**(1), 89–94 (2006)
T.D.B. Nguyen-Vu, H. Chen, A.M. Cassell, R. Andrews, M. Meyyappan, J. Li, IEEE Trans. Biomed. Engr. **54**, 1121–1128 (2007)
L. Snyder, A.J. Robinson, in *Clinical Electrophysiology: Electrotherapy and Electrophysiologic Testing*, (Williams & Wilkins, San Francisco, Neural Prostheses (Ed.: R.J. Maciunas), American Association of Neurological Surgeons 2000).
W.V. Soussou, G.J. Yoon, R.D. Brinton, T.W. Berger, IEEE Trans. Biomed. Engr. **54**, 1309–1319 (2007)
N.P. Staff, N. Spruston, Hippocampus **13**, 801–815 (2003)
T. Tominaga, Y. Tominaga, M. Ichikawa, J. Neurophysiol. **88**, 1523–1532 (2002)
K. Wang, H.A. Fishman, H. Dai, J.S. Harris, Nano Lett. **6**(9), 2043–2048 (2006)
T. Yu, S. McKinney, H.A. Lester, N. Davidson, PNAS **98**(9), 5264–5269 (2001)
Z. Yu, T.E. McKnight, M.N. Ericson, A.V. Melechko, M.L. Simpson, B. Morrison, Nano Lett. **7**(8), 2188–2195 (2007)